Spin-quantization and spin–orbit coupling effects on the line shapes of triplet states. II. The "small" exciton problem[a)]

J. P. Lemaistre[b)c)] and A. H. Zewail[d)]

Arthur Amos Noyes Laboratory of Chemical Physics,[e)] California Institute of Technology, Pasadena, California 91125

(Received 3 July 1979; accepted 24 September 1979)

This paper presents a detailed study of the effect of spin-quantization and spin–orbit coupling on the transition energies of triplet state dimers or small excitons. We consider both translationally equivalent (AA) and inequivalent (AB) dimers. For the AA and AB systems, we calculate transition frequency shifts induced by the spin–orbital coupling and by the spin–spin interactions between the *plus* (+) and *minus* (−) states of the dimer. As a result of these combined effects the *selective* coupling between the $\pm$ states of the singlet and the $\pm$ states of the triplet AA dimer system is *not* operative in the AB system. Furthermore, the role of the gas-to-crystal shifts and the intermolecular spin–spin interactions is to change the observed transition frequencies and hence cause a dispersion in the frequencies of the $\pm$ states. The relationship between such a dispersion in the AA and the same AB system is directly related to molecular parameters such as the strength of spin–orbital coupling. These results are applied to three experimental findings obtained for different dimer systems—phenazine, naphthalene, and tetrachlorobenzene dimers isolated in isotopically mixed crystals at $T < 2°K$. The phenazine results are reported here and the other data on naphthalene and tetrachlorobenzene were obtained from the literature. Agreement between theory and the recent experiments is encouragingly good.

I. INTRODUCTION

In our first publication (referred to here as I)[1] on the effect of spin–orbital coupling on the line shapes of triplet state transitions in isolated molecules, we mentioned that exciton and dimer line shapes may be influenced by the spin–orbital coupling (SOC) differently from the isolated molecule. Here we present a detailed study of the role of SOC, spin quantization (determined by, e. g., spin–other-spin and gas-to-crystal shift), and vibronic effects on the observed line shape function of "small" excitons or dimers[2] in their triplet states.

In isolated molecules it is now known that SOC influences the radiative lifetime of singlet–triplet transitions as first discussed by McClure.[3] It is also known from the work of Hochstrasser[4] that SOC makes the intensity and polarization of singlet–triplet exciton transitions different from their parentage singlet–singlet transitions. Spin–spin interactions, on the other hand, make the zero-field splittings (ZFS) of the triplet exciton different from the molecular values depending on the relative orientation of the two (or more) molecules in the unit cell of the crystal, as prescribed by Sternlicht and McConnell.[5]

Line shapes contain information about the ZFS and the dynamics of the transitions. Because dimers, or small excitons, represent the intermediate case between the single molecule limit and the "large" exciton (many molecules) limit, they have been used, theoretically and experimentally, to explore the dynamics of exciton "motion" and exciton–phonon coupling. Information is usually extracted from the linewidth of the transition, optical and magnetic, as reviewed recently by Silbey[6a] and Zewail.[6b]

The energies of the zero-field EPR transitions in dimers can be related to those of the monomer using SOC if the dimer is translationally equivalent (Zewail and Harris[7]), and using spin–spin coupling if the dimer is translationally inequivalent (Hutchison and King[8]). However, as discussed later, these effects (and others) must be considered in a unified way to describe dispersions in the translationally equivalent (henceforth referred to as AA) and especially in the translationally inequivalent (AB) dimers.[9]

Similarly, one would like to relate the homogeneous linewidth of the AA and AB dimers to that of their mother transition, the monomer. In Paper I,[1] the monomer linewidth of the zero-field EPR transitions was related to the linewidth of the optical transitions by SOC. In the dimer, new effects arise due to the excitonic coupling (between A and A or A and B molecules) which produces the *plus* and *minus* states that are linear combinations of the molecular one-site functions. Consequently, the EPR and the optical transition line shapes of the *plus* and *minus* states may or may not be different.

In this paper, we treat the effects of both spin–spin and spin–orbital couplings on the line shape (position and width) functions of the AA and AB dimers. We show that these two effects, in addition to the guest–host and the intermolecular spin–spin interactions, contribute to the line shapes of the transitions in a unique way that

[a)] This work was supported in part by grant No. DMR77-19578 from the National Science Foundation, and in part by contracts from the United States Department of Energy.

[b)] National Science Foundation (U. S. A.)–Centre National de la Recherche Scientifique (France) Visiting Postdoctoral Research Fellow.

[c)] Permanent address: Laboratoire d'Optique Moléculaire, LA 283 du CNRS, Université de Bordeaux I, 33405 Talence, France.

[d)] Alfred P. Sloan Fellow, and Camille and Henry Dreyfus Teacher-Scholar.

[e)] Contribution No. 6028.

 0021-9606/80/021055-16$01.00

depends on the orientation of the molecules involved and on the magnitude of the electronic interaction matrix element. We also show that in the AB small exciton the coupling is between *all* the states involved (± singlet and ± triplet states) even though in the AA dimer or A monomer there is only *one* channel for SOC. We apply these findings to recent experimental data obtained by us on phenazine, by Zewail and Harris[7] on 1, 2, 4, 5-tetrachlorobenzene (TCB), and by Schmidt *et al.* [10] on naphthalene dimers. This paper (II) gives the resonance position, and in Paper III[11] we discuss the width and dephasing of these small excitons.

The paper is outlined as follows: Section II is devoted to the theoretical findings, and Sec. III to the applications of the derived theoretical expressions to experimental results. Finally, in Sec. IV, we summarize the main points of the study.

II. THEORETICAL

In this section, we shall derive expressions for the perturbed energies and wave functions of the electronic states of the dimer. Specifically, we shall include the effects of both the SOC and the spin quantization on the states of AA and AB dimers. First, we treat the more complicated AB case.

A. The Hamiltonian and wave functions

Let us consider an AB dimer of two identical and translationally inequivalent molecules, A and B, as, for instance, two guest molecules embedded in their host lattice. We assume that the two molecules A and B are related by an interchange operator. The total (spin and electronic) Hamiltonian for the AB system can be written in the rigid lattice approximation as

$$H = H_O + H_P \,, \tag{2.1a}$$

with

$$H_O = H_{el}^{A} + H_d^{A} + H_{el}^{B} + H_d^{B} + H_{el}^{AB} \,, \tag{2.1b}$$

$$H_P = H_{SO}^{A} + H_{SO}^{B} \,, \tag{2.1c}$$

where $H_{el}^{A(B)}$ stand for the electronic Hamiltonian of molecule A(B); $H_d^{A(B)}$ describes the spin–spin dipolar interactions in the triplet state of molecule A(B); H_{el}^{AB} is the electronic resonance interaction Hamiltonian (reduced to the electron exchange for the triplet states) between molecules A and B; and $H_{SO}^{A(B)}$ stands for the spin–orbital Hamiltonian for the interaction between singlet (or triplet) states and the lowest triplet state in A(B). We shall treat the spin–orbital interactions H_P as a perturbation on the eigenstates of H_O.

The choice for the zero-order functions (of H_O) is dependent on the ratio of the spin–spin interaction matrix elements, determined by $H_d^{A(B)}$, to the electronic resonance interaction matrix element determined by H_{el}^{AB}.[12] Two limits may be considered. First, the case where $H_{el}^{AB} \leq H_d^{A(B)}$. Under this condition (weak or intermediate coupling between A and B), the spin–electronic eigenstates of H_O are obtained from the diagonalization of the full energy matrix (6×6) written for instance, in the delocalized basis set or in the one-site basis set.[7a] The total wave function describing the two triplet dimer states cannot therefore be written as simple products of electronic and spin functions. The second case is when $H_{el}^{AB} \gg H_d^{A(B)}$. In this limit (strong coupling), the triplet spin functions for the dimer are generated from spin Hamiltonian operators calculated for each delocalized excited electronic state, i. e., the eigenstate of $H_{el}^{A} + H_{el}^{B} + H_{el}^{AB}$.

In the work discussed here, the *plus* and *minus* states (±) are optically and magnetically separable from the monomer state. Hence, we shall consider only the case where $H_{el}^{AB} \gg H_d^{A(B)}$ and for which the electronic resonance interaction between the two molecules is larger than the zero-field splittings in the triplet state of each molecule.

Let us denote by ϕ_0^i, $^1\phi^i$, and $^3\phi^i$ $(i = A, B)$ the orbital wave functions describing each molecule in the ground state, in the excited singlet state, and in the excited triplet state of interest, respectively. We shall denote by ϕ_0, $^1\phi_\pm$, $^3\phi_\pm$ the electronic representations of $H_{el}^{A} + H_{el}^{B} + H_{el}^{AB}$ for the ground state, singlet excited states, and triplet excited states of the AB dimer, respectively. Assuming that the resonance condition between the excited sites (A or B) is satisfied, the orbital–spin wave functions for the dimer states involved can be written as

$$|\phi_0\rangle = |\phi_0^A \phi_0^B \sigma_{s_0}\rangle \,, \tag{2.2a}$$

$$|{}^1\phi_\pm \sigma_s\rangle = (1/\sqrt{2})\,|[{}^1\phi^A \phi_0^B \pm \phi_0^A\, {}^1\phi^B]\sigma_s\rangle \tag{2.2b}$$

$$|{}^3\phi_\pm \sigma_M^\pm\rangle = (1/\sqrt{2})\,|[{}^3\phi^A \phi_0^B \pm \phi_0^A\, {}^3\phi^B]\sigma_M^\pm\rangle \,, \tag{2.2c}$$

where σ_{s_0} and σ_s stand for the spin functions of the ground state and the singlet state of the dimer, and $\sigma_M^\pm$ are the three triplet spin functions for each delocalized state (±) of the dimer. $\hat{M}$ are the spin magnetic axes (polarization) and M denotes the magnetic energies of the triplet spin quantized along these axes. The form of the $\sigma_M^\pm$ functions can be obtained after the integration of the total spin–spin dipolar Hamiltonian, $H_d^A + H_d^B$, over the electronic wave function of the (±) states of the dimer. The resultant spin Hamiltonian determines the properties of $\sigma_M^\pm$ which are related to the monomer wave function (see the coming section). For the monomer (A or B molecule), the spin Hamiltonian is simply

$$H_S^{A(B)} = -[XS_X^2 + YS_Y^2 + ZS_Z^2] \,, \tag{2.3}$$

where S_X, S_Y, S_Z are the triplet spin angular momentum operators along the principal axes $(\hat{X}, \hat{Y}, \hat{Z})$ of the molecule and X, Y, Z are therefore the energies of the three magnetic sublevels.

B. The perturbed states: symmetric and antisymmetric interactions

Let us consider the strong coupling limit case for which the electronic resonance interaction (H^{AB}) between the two molecules is larger than the intramolecular spin–spin dipolar interactions ($H_d^{A(B)}$). A complete basis set of spin–electronic functions for the dimer can be chosen as $|{}^3\phi_\pm \sigma_M^\pm\rangle$ of Eq. (2.2c), in which the orbital parts describe the two electronic states with the energies $E_0^T \pm J_T$. In these dimer states the triplet spins represented by the $\sigma_M^\pm$ functions are quantized along the $\hat{M}(X^*, Y^*, Z^* \equiv b)$ axes.

In order to get the spin Hamiltonian in each delocalized state ${}^3\phi_\pm$, we perform the integration of the total Hamiltonian (orbital + spin) for the dimer over the electronic coordinates of A and B. This leads to two kinds of matrix elements:

$$\text{(i)}\ \langle\sigma_M^\pm|\langle{}^3\phi_\pm|H_{el}^A+H_{el}^B+H_{el}^{AB}+H_d^A+H_d^B|{}^3\phi_\pm\rangle|\sigma_{M'}^\pm\rangle$$
$$=\langle\sigma_M^\pm|(E_0^T\pm J_T+\tfrac{1}{2}(H_S^A+H_S^B)|\sigma_{M'}^\pm\rangle\ , \qquad (2.4a)$$

$$\text{(ii)}\ \langle\sigma_M^\pm|\langle{}^3\phi_\pm|H_{el}^A+H_{el}^B+H_{el}^{AB}+H_d^A+H_d^B|{}^3\phi_\mp\rangle|\sigma_{M'}^\mp\rangle$$
$$=\langle\sigma_M^\pm|\tfrac{1}{2}(H_S^A-H_S^B)|\sigma_{M'}^\mp\rangle\ . \qquad (2.4b)$$

In (2.4), H_S^i $(i=\text{A, B})$ is the molecular spin Hamiltonian describing the spin–spin interactions in the triplet state of the molecule and is given by Eq. (2.3).

In the strong coupling limit that we are considering, the second type of matrix elements [Eq. (2.4b)] are small compared to the energy difference ($\simeq 2J_T$) between the *plus* and *minus* states and can be treated as perturbation terms. Neglecting these *plus–minus* coupling terms in a zero-order approximation, the eigenspin functions of $\frac{1}{2}(H_S^A+H_S^B)$ together with the ${}^3\phi_\pm$ orbital functions diagonalize the full spin–electronic Hamiltonian. Furthermore, in the absence of such coupling the magnetic axes in the (±) states are identical and we can choose the same basis set of spin functions for both (±) states ($\sigma_M\equiv\sigma_M^+\equiv\sigma_M^-$). We now choose the crystal axes system as a common (to A and B) coordinate system to express H_S^A and H_S^B. In the abc' orthonormal frame, $H_S^{A(B)}$ can be written as

$$H_S^{A(B)}=-(BS_b^2+AS_a^2+C'S_{c'}^2+\alpha_{ac'}(S_aS_{c'}+S_{c'}S_a)$$
$$\pm\alpha_{ab}(S_aS_b+S_bS_a)\pm\alpha_{bc'}(S_bS_{c'}+S_{c'}S_b))\ . \qquad (2.5)$$

In (2.5), S_b, S_a, $S_{c'}$ are the triplet spin angular momentum operators along the crystal axes. The interchange of A and B with an operator along the b axis leaves the molecules unchanged (symmetrical operation). The parameters B, A, C' and α's in the spin Hamiltonians [Eq. (2.5)] are related to the molecular zero-field splittings by means of the direction cosines $(\hat{M}\cdot\hat{m})$ of the molecular axes $(\hat{m})$ onto the crystal axes $(\hat{M})$ (note that the molecular axes and the dipolar interaction principal axes are parallel for high symmetry molecules like the ones we are considering here):

$$M=\sum_m m(\hat{M}\cdot\hat{m})^2\ , \qquad (2.6a)$$

$$\alpha_{MM'}=\sum_m m(\hat{M}\cdot\hat{m})(\hat{M}'\cdot\hat{m})$$
$$(m=X,Y,Z;M=A,B,C';\hat{M}=a,b,c')\ . \qquad (2.6b)$$

Taking the sum of $H_S^{A(B)}$ in Eq. (2.5), we have

$$(1/2)(H_S^A+H_S^B)=H_S^b$$
$$=-(BS_b^2+AS_a^2+C'S_{c'}^2+\alpha_{ac'}(S_aS_{c'}+S_{c'}S_a)), \qquad (2.7)$$

which is totally symmetric under the C_2 rotation along the b axis. Now, in order to get a diagonal form for H_S^b, we perform a rotation θ in the ac' plane around the b axis. Such a rotation defines new spin operators S_{X^*}, S_{Y^*}:

$$S_a=\cos\theta S_{X^*}-\sin\theta S_{Y^*}\ ,$$
$$S_{c'}=\sin\theta S_{X^*}+\cos\theta S_{Y^*}\ . \qquad (2.8)$$

Expressed in this axes system with $b\equiv Z^*$, $(X^*,a)=\theta$ and Y^* orthonormal to b and X^*, H_S^b becomes

$$H_S^b=-(X^*S_{X^*}^2+Y^*S_{Y^*}^2+BS_b^2$$
$$+\alpha_{X^*Y^*}(S_{X^*}S_{Y^*}+S_{Y^*}S_{X^*}))\ , \qquad (2.9a)$$

with

$$X^*=A\cos^2\theta+C'\sin^2\theta+\alpha_{ac'}\sin2\theta\ ,$$
$$Y^*=A\sin^2\theta+C'\cos^2\theta-\alpha_{ac'}\sin2\theta\ . \qquad (2.9b)$$

The condition $\alpha_{X^*Y^*}=0$ gives a diagonal form to H_S^b and allows us to calculate θ by using the following relation:

$$\theta=(1/2)\tan^{-1}(2\alpha_{ac'}/(A-C'))\ . \qquad (2.9c)$$

The above equation which utilizes *only* the symmetric part of the Hamiltonian, H_S^b, is identical to the result of Ref. 5 which ignores (for good reason) the antisymmetric part, $H_S^{ac'}$, that we treat next.

The spin operator which couples the triplet *plus* and *minus* states of the AB dimer as shown in (2.4b) is given by the difference between H_S^A and H_S^B of Eq. (2.5):

$$H_S^{ac'}=(1/2)(H_S^A-H_S^B)$$
$$=-(\alpha_{ab}(S_aS_b+S_bS_a)+\alpha_{bc'}(S_bS_{c'}+S_{c'}S_b))\ . \qquad (2.10)$$

Expressed in the dimer frame, this Hamiltonian now takes the following useful form:

$$H_S^{ac'}=-(t_{X^*b}(S_{X^*}S_b+S_bS_{X^*})+t_{Y^*b}(S_{Y^*}S_b+S_bS_{Y^*}))\ , \qquad (2.11a)$$

with

$$t_{X^*b}=\alpha_{ab}\cos\theta+\alpha_{bc'}\sin\theta\ ,$$
$$t_{Y^*b}=-\alpha_{ab}\sin\theta+\alpha_{bc'}\cos\theta\ . \qquad (2.11b)$$

Through the knowledge of θ and α we utilize this Hamiltonian to calculate matrix elements of Eq. (2.4) which we shall use later.

Finally, with the above basis set of Eq. (2.2c),

$$\langle{}^3\phi_\pm\sigma_M|H_{el}^A+H_{el}^B+H_{el}^{AB}+H_S^A+H_S^B|{}^3\phi_\pm\sigma_{M'}\rangle$$
$$=\left(E_{A(B)}+\sum_m m(\hat{M}\cdot\hat{m})^2\pm J_T\right)\delta_{MM'} \qquad (2.12a)$$

and

$$\langle{}^3\phi_\pm\sigma_M|H_{el}^A+H_{el}^B+H_{el}^{AB}+H_S^A+H_S^B|{}^3\phi_\mp\sigma_{M'}\rangle$$
$$=(1/2)\sum_m m[(\hat{M}'\cdot\hat{m}_A)(\hat{M}\cdot\hat{m}_A)-(\hat{M}'\cdot\hat{m}_B)(\hat{M}\cdot\hat{m}_B)]\ . \qquad (2.12b)$$

For $M=M'$, the matrix element in Eq. (2.12b) is zero. Therefore, ${}^3\phi_\pm\sigma_M$ are eigenfunctions of the *entire* Hamiltonian when we ignore the small off-diagonal terms determined by the mixing of *plus* and *minus* states with the *minus* and *plus* states through $H_S^{ac'}$.

From above we see that H_S^b is a zero-order spin Hamiltonian for the small exciton states and that $H_S^{ac'}$ *is the operator which couples the plus and minus states.* H_S^b and $H_S^{ac'}$ are given in terms of H_S^A and H_S^B according to Eqs. (2.7) and (2.10), which utilize the symmetry of the unit cell. Again using the symmetry operation be-

tween A and B, we may similarly separate the monomer SOC matrix element into symmetric and antisymmetric parts[4]

$$(H_{SO}^{b})_{eff} = \langle H_{SO}^{b} \rangle_{\pm\pm} \equiv \langle H_{SO}^{A} + H_{SO}^{B} \rangle_{\pm\pm} , \quad (2.13a)$$

$$(H_{SO}^{ac'})_{eff} = \langle H_{SO}^{ac'} \rangle_{\pm\mp} \equiv \langle H_{SO}^{A} + H_{SO}^{B} \rangle_{\pm\mp} . \quad (2.13b)$$

As we shall see in more detail later, H_{SO}^{b} couples singlet and triplet states with the same orbital symmetry while $H_{SO}^{ac'}$ couples singlet and triplet states with opposite orbital symmetry.

As a result of the interaction between the *plus* and *minus* states through $H_S^{ac'}$, we have two different sets of triplet spin functions denoted by $\sigma_M^{\pm}$. Considering that $H_S^{ac'}$ is a small perturbation term, a good representation of these functions is given by the eigenfunctions of H_S^{b}:

$$H_S^{b} |\sigma_M\rangle = M |\sigma_M\rangle \quad (2.14a)$$

$$|\sigma_M^{+}\rangle \equiv |\sigma_M^{-}\rangle \equiv |\sigma_M\rangle . \quad (2.14b)$$

Hence, in this case $\hat{M} = X^*, Y^*, Z^*$, with the asterisk denoting the quantization axes for the AB dimer in the absence of $H_S^{ac'}$ perturbation. This perturbation together with the spin–orbital perturbation now defines H_P of Eq. (2.1): H_P couples the $+(-)$ triplet state to (i) the singlet $+(-)$ state by H_{SO}^{b}; (ii) the singlet $-(+)$ state by H_{SO}^{ac}; and (iii) the $-(+)$ triplet state by $H_S^{ac'}$.

C. General expressions

Now that we know the eigenfunctions of H_O, the perturbed (unnormalized) triplet wave function as a result of H_P can be written as

$$|{}^3\psi_{\pm}^{M}\rangle = |{}^3\phi_{\pm}\sigma_M\rangle - \lambda_{\pm\pm}^{M} |{}^1\phi_{\pm}\sigma_S\rangle - \lambda_{\mp\pm}^{M} |{}^1\phi_{\mp}\sigma_S\rangle + \sum_{M'} \lambda^{MM'} |{}^3\phi_{\mp}\sigma_{M'}\rangle . \quad (2.15)$$

In Eq. (2.15), ϕ are the orbital wave functions in the absence of the perturbation and ψ denotes the total wavefunction. As in Paper I, we assume a two-electron state on each molecule; thus, we may write the spin–electronic functions as products of the spin and electronic wave functions. The effect of SOC is simply to mix these product functions of the singlet and triplet states. $\lambda_{\pm\pm}^{M}$ is the spin–orbital mixing (by H_{SO}^{b}) coefficient between $+(-)$ of the triplet and $+(-)$ of the singlet for the specific $\hat{M}(X^*, Y^*, Z^*)$ state. Similarly, $\lambda_{\mp\pm}^{M}$ is the spin–orbital coefficient for mixing (by $H_{SO}^{ac'}$) the $+(-)$ state of the triplet with the $-(+)$ state of the singlet. (Note that the lowest triplet–higher-triplet mixing by SOC can be handled similarly.) The last coefficient $\lambda^{MM'}$ in Eq. (2.15) is to describe the coupling between $+$ and $-$ states of the lowest triplet state. This coupling involves all spin states M and $M'(X^*, Y^*, Z^*)$. With this in mind we can now write these coefficients explicitly, using perturbation theory, as

$$\lambda_{\pm\pm}^{M} = \tau_{\pm\pm}/(\Delta - M \pm (J_s - J_T)) , \quad (2.16a)$$

$$\lambda_{\mp\pm}^{M} = \tau_{\mp\pm}/(\Delta - M \mp (J_s + J_T)) , \quad (2.16b)$$

$$\lambda^{MM'} = t_{MM'}/(M - M' \pm 2J_T) , \quad (2.16c)$$

where $\Delta = E_O^S - E_O^T$ is the difference between the zero-order energies of singlet and triplet states. M is the energy of the spin state and J_S and J_T are, respectively, the singlet and triplet electronic interaction matrix elements between the two molecules. The matrix element for the spin–orbital operator between the $+(-)$ of the triplet and the $+(-)$ of the singlet through H_{SO}^{b} is $\tau_{\pm\pm}^{M}$, while that between the $+(-)$ of the triplet and the $-(+)$ of the singlet through $H_{SO}^{ac'}$ is $\tau_{\mp\pm}^{M}$. Finally, $t_{MM'}$ is for triplet plus and minus states coupling [see Eqs. (2.11)]

$$\tau_{\pm\pm}^{M} = \langle {}^1\phi_{\pm}\sigma_S | H_{SO}^{A} + H_{SO}^{B} | {}^3\phi_{\pm}\sigma_M \rangle , \quad (2.17a)$$

$$\tau_{\mp\pm}^{M} = \langle {}^1\phi_{\mp}\sigma_S | H_{SO}^{A} + H_{SO}^{B} | {}^3\phi_{\pm}\sigma_M \rangle , \quad (2.17b)$$

$$t_{MM'} = \langle {}^3\phi_{\mp}\sigma_{M'} | H_S^{ac'} | {}^3\phi_{\pm}\sigma_M \rangle . \quad (2.17c)$$

The choice of the basis functions in the above equations stems from the fact that both the spin–spin and spin–orbital interactions are small relative to J_S and J_T. One may also use other basis sets, for example, one where the spin–orbital mixing is in the one-site function of A and B[7a] (see Appendix A).

The energies of the six perturbed triplet states can now readily be obtained from Eqs. (2.15)–(2.17). These are

$$E_{\pm M}^{T} = E_O^{T} + M \pm J_T - |\lambda_{\pm\pm}^{M}|^2 [\Delta - M \pm (J_S - J_T)] - |\lambda_{\mp\pm}^{M}|^2 [\Delta - M \mp (J_S + J_T)] + \sum_{M'} |\lambda^{MM'}|^2 [M - M' \pm 2J_T] . \quad (2.18)$$

Using Eq. (2.18) and neglecting (i) the zero-field energies (splittings) compared to the energy difference between the singlet and triplet states, (ii) the differences $M - M'$ compared to J_T, we get a simple expression for the three zero-field EPR frequencies in each dimer state:

$$\hbar\omega_{MM'}^{\pm} = (M - M') - (|\tau_{\pm\pm}^{M}|^2 - |\tau_{\pm\pm}^{M'}|^2)/(\Delta \pm (J_S - J_T)) - (|\tau_{\mp\pm}^{M}|^2 - |\tau_{\mp\pm}^{M'}|^2)/(\Delta \mp (J_S + J_T)) + \sum_{M''} (|t_{MM''}|^2 - |t_{M'M''}|^2)/\pm 2J_T . \quad (2.19)$$

The above Eq. (2.19) demonstrates the effect of *both* the spin–orbital as well as the spin–spin mixing on the observed transition frequencies $\omega_{MM'}^{\pm}$ in the $(\pm)$ states. Several things are noted. First, the coupling between the $+(-)$ and $-(+)$ states cannot be neglected, especially when the energy denominators in the second and third terms of Eq. (2.19) are favorable. This point has an important implication: In general, we therefore expect *the mixing of the singlet band with the triplet band through* SOC *to make the k-to-k (where k is the wave vector of the exciton) interactions nonselective.* In other words, through the $H_{SO}^{ac'}$ perturbation k of the singlet state may interact with k' of the triplet state (not k only) leading to a complicated band-to-band EPR transition. Second, the spin–spin mixing may disperse or narrow the difference (due to the SOC) in frequencies between the *plus* and *minus* states depending on the sign of J_T and the relative magnitude of $t_{MM''}$ and $t_{M'M''}$.

D. Geometrical effects in the AB system

Here, we shall consider the dependence of the energies of the transitions on the relative orientation of A

and B molecules using the results of the previous section. This geometrical effect is included in the zero order spin functions of the *plus* and *minus* states of the AB dimer. The σ_M, which are identical in the + and − states provided that H_S^{so} effect is small, can be written as linear combinations of the molecular triplet spin functions σ_m^i:

$$|\sigma_M\rangle = \sum_m (\hat{M}\cdot\hat{m}_i)|\sigma_m^i\rangle \ ; \quad (i=\mathrm{A,B};\hat{m}=X,Y,Z)\ , \tag{2.20}$$

where the $(\hat{M}\cdot\hat{m}_i)$ are the direction cosines of the dimer axes $(\hat{M}=X^*, Y^*, Z^*)$ with respect to the molecular $\hat{m}_i$ axes of A or B. This last step allows us to rewrite the six triplet spin functions [Eq. (2.2c)] for the AB dimer as follows:

$$|^3\phi_\pm\sigma_M\rangle = (1/\sqrt{2})\left\{\left|{}^3\phi^{\mathrm{A}}\phi_0^{\mathrm{B}}\sigma_{s_0}^{\mathrm{B}}\sum_m(\hat{M}\cdot\hat{m}_{\mathrm{A}})\sigma_m^{\mathrm{A}}\right\rangle \pm \left|\phi_0^{\mathrm{A}}\,{}^3\phi^{\mathrm{B}}\sigma_{s_0}^{\mathrm{A}}\sum_m(\hat{M}\cdot\hat{m}_{\mathrm{B}})\sigma_m^{\mathrm{B}}\right\rangle\right\}\ . \tag{2.21}$$

The energies of these functions in terms of the direction cosines are given in Eq. (2.6a). The SOC matrix elements [Eq. (2.17a) and (2.17b)] between singlet and triplet states can now be easily calculated. Using Eqs. (2.21) and (2.17), we get

$$\tau_{\pm\pm}^M = (1/2)\sum_m \tau^m((\hat{M}\cdot\hat{m}_{\mathrm{A}})+(\hat{M}\cdot\hat{m}_{\mathrm{B}}))\ , \tag{2.22a}$$

$$\tau_{\mp\pm}^M = (1/2)\sum_m \tau^m((\hat{M}\cdot\hat{m}_{\mathrm{A}})-(\hat{M}\cdot\hat{m}_{\mathrm{B}}))\ . \tag{2.22b}$$

In Eqs. (2.22a) and (2.22b), τ^m is the molecular SOC matrix element for the mth sublevel which is identical for both molecules, A and B:

$$\tau_i^m = \langle {}^1\phi^i\sigma_s^i|H_{\mathrm{SO}}^i|{}^3\phi^i\sigma_m^i\rangle \quad (i=\mathrm{A,B})\ . \tag{2.22c}$$

Owing to the fact that $Z^*\equiv b$ is a twofold symmetry axis, we have

$$(\hat{M}\cdot\hat{m}_{\mathrm{B}}) = -(\hat{M}\cdot\hat{m}_{\mathrm{A}}) = -(\hat{M}\cdot\hat{m}) \quad \text{if } \hat{M}=X^*, Y^* \tag{2.23a}$$

and

$$(\hat{M}\cdot\hat{m}_{\mathrm{B}}) = (\hat{M}\cdot\hat{m}_{\mathrm{A}}) = (\hat{M}\cdot\hat{m}) \quad \text{if } \hat{M}=b\ . \tag{2.23b}$$

This symmetry consideration leads to the following relationships:

$$\tau_{\pm\pm}^{X^*} = \tau_{\pm\pm}^{Y^*} = 0\ , \quad \tau_{\pm\pm}^b = \sum_m \tau^m(\hat{b}\cdot\hat{m})\ , \tag{2.24a}$$

$$\tau_{\mp\pm}^{X^*} = \sum_m \tau^m(\hat{X}^*\cdot\hat{m})\ , \quad \tau_{\mp\pm}^{\hat{Y}^*} = \sum_m \tau^m(\hat{Y}^*\cdot\hat{m})\ , \quad \tau_{\mp\pm}^b = 0\ . \tag{2.24b}$$

Knowledge of the coefficients in Eq. (2.24), together with $t_{M\mu'}$ [as derived in Eq. (2.11)] enables us to calculate the energy shifts induced by SOC and spin–spin mixings for each triplet sublevel:

$$\Delta_M^\pm = -|\tau^m|^2(\hat{M}\cdot\hat{m})^2/(\Delta\mp(J_S+J_T)) + |t_{Mb}|^2/\pm 2J_T \quad (M=X^*, Y^*) \tag{2.25a}$$

and

$$\Delta_b^\pm = -|\tau^m|^2(\hat{b}\cdot\hat{m})^2/(\Delta\pm(J_S-J_T)) + (|t_{X^*b}|^2+|t_{Y^*b}|^2)/\pm 2J_T\ . \tag{2.25b}$$

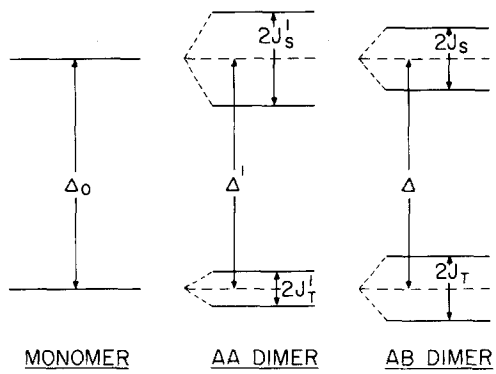

FIG. 1. A schematic describing the splitting discussed in the text for the AB, AA, and A systems.

In Eq. (2.25), we have assumed that only one spin–orbit route (m) in the molecule couples the singlet with the triplet state. However, the above results indicate that even with one molecular active spin state, the AB dimer will show *multiple* routes for the coupling, hence changing the line shape properties from those of the monomer and the AA dimer.

The SOC contributions to the energy shifts involve expressions like

$$|\tau^m|^2/(\Delta\pm(J_S-J_T)) \tag{2.26a}$$

if we neglect the guest–host shifts. It has been established that in isotopic mixed crystals like naphthalene[13] and phenazine,[14] the guest–host energy shifts in triplet dimers (AA or AB) are different from the monomer. The shift $\Delta-\Delta_0$ (i.e., the difference in energy between the singlet–triplet splitting of the AB dimer *minus* the singlet–triplet splitting of the monomer in the crystal) may be introduced in Eq. (2.26a) within the framework of perturbation theory. Assuming that Δ_0 (see Fig. 1) is larger compared to $(\Delta-\Delta_0)$ and J_S, J_T, we get instead of Eq. (2.26a) the following expression:

$$\frac{|\tau^m|^2}{\Delta_0}\left(1-\frac{\Delta-\Delta_0}{\Delta_0}\pm\frac{J_S-J_T}{\Delta_0}\right)\ . \tag{2.26b}$$

The above correction terms may therefore induce *asymmetric* shifts for the spin sublevels of dimers around the monomer.

Finally, with the relations [Eq. (2.25)], we get the following dispersion (i.e., the difference in transition energies between the *plus* and the *minus* states; $\Delta_M = \Delta_M^+ - \Delta_M^-$) introduced by the SOC:

$$(\Delta_M)_{\mathrm{SOC}} = -2|\tau^m|^2(\hat{M}\cdot\hat{m})^2(J_S+J_T)/\Delta^2 \quad (M=X^*, Y^*)\ , \tag{2.27a}$$

$$(\Delta_b)_{\mathrm{SOC}} = 2|\tau^m|^2(\hat{b}\cdot\hat{m})^2(J_S-J_T)/\Delta^2\ , \tag{2.27b}$$

and by the spin–spin mixing:

$$(\Delta_M)_{\mathrm{Sp-Sp}} = |t_{Mb}|^2/J_T \quad (\hat{M}=X^*, Y^*)\ , \tag{2.27c}$$

$$(\Delta_b)_{\mathrm{Sp-Sp}} = (|t_{X^*b}|^2+|t_{Y^*b}|^2)/J_T\ . \tag{2.27d}$$

E. The AA system

The calculation of the perturbed triplet spin functions for translationally equivalent dimers is greatly simpli-

fied because the axes of the two molecules A_1 and A_2 are parallel. The triplet spin functions in each state of the A_1A_2 dimer are identical to those of the monomer since from Eq. (2.21) we must now have

$$|{}^3\phi_\pm\sigma_m\rangle = (1/\sqrt{2})(|{}^3\phi^{A_1}\phi_0^{A_2}\sigma_m^{A_1}\sigma_{s_0}^{A_2}\rangle \pm |\phi_0^{A_1}{}^3\phi^{A_2}\sigma_{s_0}^{A_1}\sigma_m^{A_2}\rangle) . \quad (2.28)$$

Due to the fact that the two spin Hamiltonians of A_1 and A_2 commute, the off-diagonal matrix elements of the spin–spin interaction operator ($H_S^{ac'}$), which couple the *plus* and *minus* states in the AB dimer case, cancel in this case. So, the spin–spin mixing effects of AB dimers do not exist in the AA system, and consequently will not introduce a difference in the zero-field EPR frequencies in such systems. However, the spin–orbital and spin (on A_1)–spin (on A_2) interactions can introduce such a disparity.

The singlet states involved in the SOC can now be written as

$$|{}^1\phi_\pm\sigma_s\rangle = (1/\sqrt{2})|({}^1\phi^{A_1}\phi_0^{A_2} \pm \phi_0^{A_1}{}^1\phi^{A_2})\sigma_s\rangle . \quad (2.29)$$

The application of Eq. (2.22) to the case of two parallel molecules obviously shows that $\tau_{\pm\pm}^m = \tau^m$ and $\tau_{\mp\pm} = 0$, where τ^m is the molecular spin–orbit matrix element. In other words, the SOC matrix elements between the singlet and the triplet dimer states having different symmetries also cancel.

Bearing in mind these simplifications, the coupling between the symmetric (antisymmetric) triplet spin sublevels and the symmetric (antisymmetric) singlet states produces the following perturbed functions:

$$|{}^3\psi_\pm^m\rangle = |{}^3\phi_\pm\sigma_m\rangle - \lambda'^m|{}^1\phi_\pm\sigma_s\rangle , \quad (2.30a)$$

with

$$\lambda_\pm'^m = \tau^m/(\Delta' - m \pm (J_S' - J_T')) . \quad (2.30b)$$

The primed terms in Eq. (2.30) have the same definition as that of the AB system. Neglecting m energies compared to Δ', the level shifts in the spin states of the AA dimer are simply given by

$$\Delta_m^\pm = -|\tau^m|^2/(\Delta' \pm (J_S' - J_T')) . \quad (2.31)$$

With the condition that $|J_S' - J_T'| \ll \Delta'$, the relation in Eq. (2.31) leads finally to the following energy dispersion:

$$(\Delta_m)_{SOC} = \Delta_m^+ - \Delta_m^- = 2|\tau^m|^2(J_S' - J_T')/\Delta'^2 , \quad (2.32)$$

which is identical to Eq. (7) of Ref. 7(b), derived for the case of translationally equivalent dimers.

F. Relationships between the energy dispersion in AA and AB systems

By comparing Eqs. (2.27) and (2.32), one notices that the spin–orbital effects in the AB dimer are related to that of the AA dimer made of the "same" molecules. The ratio of the differences in the energy shifts between the *plus* and *minus* states in AB dimers relative to the AA dimer is

$$(\Delta_M)_{SOC}/(\Delta_m)_{SOC} = -(\hat{M}\cdot\hat{m})^2(\Delta'/\Delta)^2(J_S + J_T)/(J_S' - J_T') \quad (M = X^*, Y^*) \quad (2.33a)$$

and

$$(\Delta_b)_{SOC}/(\Delta_m)_{SOC} = (\hat{b}\cdot\hat{m})^2(\Delta'/\Delta)^2(J_S - J_T)/(J_S' - J_T') . \quad (2.33b)$$

We do not include the guest–host coupling effects discussed before, so we may write $\Delta' = \Delta = \Delta_0$. Defining the ratios of the electronic resonance interaction matrix elements as

$$K = (J_S + J_T)/(J_S' - J_T') , \quad (2.34a)$$

$$K' = (J_S - J_T)/(J_S' - J_T') , \quad (2.34b)$$

we can calculate the differences in the energy shifts between the *plus* and *minus* states of the AB dimer as a function of the shifts in the AA system. We get the following useful relationships:

$$(\Delta_M)_{SOC} = -K(\Delta_m)_{SOC}(\hat{M}\cdot\hat{m})^2 \quad (M = X^*, Y^*) , \quad (2.35a)$$

$$(\Delta_b)_{SOC} = K'(\Delta_m)_{SOC}(\hat{b}\cdot\hat{m})^2 , \quad (2.35b)$$

that we shall use later.

III. APPLICATIONS TO EXPERIMENTS

A. Phenazine

In contrast with other systems, phenazine offers an opportunity to study the above mentioned effects. This is because the monomer and dimer optical spectra are separated and the ODMR can be observed on each emission.

1. Resonance and quasiresonance interactions

The triplet state resonance interactions in phenazine crystals are essentially two dimensional and strongly anisotropic.[15,16] Because the trap depths of monomers and dimers are relatively small, quasiresonance interactions with the host make the observed dimer–monomer splitting not equal to J_T'. The corrected (see Appendix B) J_T' value for the AA interaction is $J_T' = -6.5 \pm 0.8$ cm^{-1} in the isotopically mixed crystals (see also Fig. 11 and Table XI). This corrected value is important for the calculation of the dispersion in the ZFS.

The pure crystal Davydov splitting is 4 cm^{-1}.[16] This leads to a matrix element for the AB coupling of $J_T = +0.5$ cm^{-1}. Thus, the ratio of the b axis (assigned from calculation) translationally equivalent interaction to the inequivalent (ab plane) interaction is 13, while the ratio of the total translationally equivalent to inequivalent bandwidth is 6.5.

2. ODMR of monomers and AA dimers: Effect of SOC

Three isotopically mixed crystals with different perproto guest concentrations of 0.5%, 2%, and 3% (by weight) were used in these studies. All these crystals were grown from the melt by standard Bridgman techniques. Care was taken to avoid the penetration of oxygen to these crystals. Fresh crystals were used only once unless they were regrown under vacuum. When the crystal was exposed to air, say for a week, the desired portion from the ingot was put into a glass tube and degassed for at least 10 min, then mounted in the helix. No observed changes were seen in the optical spectra.

The crystals were mounted in the microwave helix

TABLE I. ODMR transition frequencies (MHz) of phenazine isotopically mixed crystals at ~1.5 K—0.5% crystal.

	(0 dB)[a]	(−20 dB)	(−30 dB)
$\|D\|+\|E\|$	(a) 2556.16 (b) 2559.59 (c) 2561.94 (Strongest) (d) 2564.93 (e) 2567.74 (f) 2571.03	Same	Only c and d
	(0 dB)	(−10 dB)	
$2\|E\|$	634.85 635.39 637.34 638.30 640.83 641.48 (Strongest) 642.42 643.06 643.72 646.22 646.90 648.95	Same	

[a]Microwave output power ranged from 0.4 to 1.3 W, $S/N \sim 30$, slit = 300 μ.

TABLE III. ODMR transition frequencies (MHz) of the strongest line in different runs and crystals of isotopically mixed phenazine crystals.

		Monomer optical emission[a]		Dimer optical emission	
$\|D\|+\|E\|$	A	2561.94 2562.3 2562.2 2562.1	2562.21 ±0.14	2563.2 2563.9 2563.4 2563.3	2563.52 ±0.31
	B	2562.36		2564.0	
	C	2562.34 2562.26		2563.3	
$2\|E\|$		641.48 641.3 641.5 640.55 640.3 640.1	640.87 ±0.57	638.2 638.1 637.93 637.9	638.03 ±0.12

[a]A: different runs on the same crystal; B and C are different crystals.

(grease free) and a 100 W mercury lamp with the appropriate filters were used for the excitation. Cooling the red-sensitive (EMI 9558) photomultiplier to −20 °C and the crystal to <2 K improved the S/N ratio considerably. The detection of the ODMR signals was done in the conventional way.[7b,14]

In Tables I–III and Figs. 2 and 3, we summarize the experimental findings of the ODMR of the differently doped crystals. The multiple peaks observed in the monomer and dimer spectra are due to the hyperfine coupling between the electron spin ($S=1$) and the nitrogen and hydrogen nuclei. Taking the strongest line in the the spectra (see Fig. 3) as the "pure" electron spin transition, we arrive at the following values for the zero-field splittings (in MHz):

$$\begin{aligned} \omega_{XZ} &= 2562.2 \pm 0.2\ , \\ \omega_{YZ} &= 1921.3 \quad \text{(monomer)}\ , \\ \omega_{XY} &= 640.9 \pm 0.6\ , \end{aligned} \tag{3.1}$$

and

$$\begin{aligned} \omega_{XZ} &= 2563.5 \pm 0.3\ , \\ \omega_{YZ} &= 1925.5 \quad \text{(AA dimer)}\ , \\ \omega_{YX} &= 638.0 \pm 0.2\ . \end{aligned} \tag{3.2}$$

TABLE II. ODMR transition frequencies (MHz) of phenazine isotopically mixed crystals at ~1.5 K—2% crystal.

		Monomer optical emission		Dimer optical emission
$\|D\|+\|E\|$	0 dB[a]	2562.3 (Very strong) 2565.9		2563.2 (Very strong) 2565.9
	−10 dB	2562.2		2563.9
	−20 dB	2562.1 2566.0		2563.4; 2563.3 (Another trace) 2565.2
$2\|E\|$	0 dB[b]	634.2 634.8 635.4 636.1 637.4 639.1 641.3; 641.5 (Another trace); Strongest 643.2	−20 dB	630.7 631.7 632.5 633.5 635.2 638.2; 638.1 (Another trace); Strongest 641.2 643.7 645.2 646.4 647.7 649.7

[a]Microwave output power 24 mW; 50% modulation at 100 Hz, 70 μ slit. At −6 dB, there appears to be some out of phase (to the main electron spin transition) signals, but the signal-to-noise ratio was good enough to resolve detailed structure.

[b]At 50% modulation depth the output power is 0.15 W.

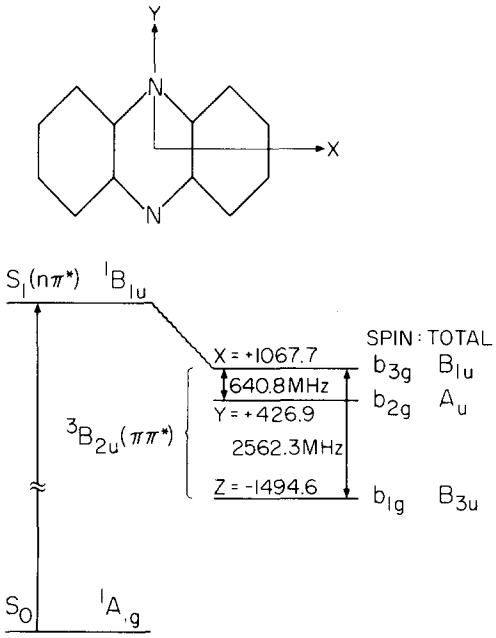

FIG. 2. The ZFS, the coordinate system, and the ordering of the three spin sublevels for the phenazine molecule.

The ordering of the spin sublevels was taken from Refs. 17 and 19 for phenazine isolated in biphenyl crystal or in a glass.

In phenazine, the lowest $T_1(\text{III}^*)$ triplet state couples to the nearby singlet states $S_1(n\Pi^*)$ [18] by SOC. In the D_{2h} symmetry point group, the orbital symmetries are $^3B_{2u}$ for T_1 and $^1B_{1u}$ for S_1 [19] (see Fig. 2 for the axis system used here). The total symmetry (orbital ⊗spin) for the three spin sublevels σ_X, σ_Y, σ_Z are respectively B_{1u}, A_u, B_{3u}. Only the σ_X triplet sublevel therefore spin–orbitally couples directly to the $^1B_{1u}$. The splitting S_1–T_1 is $\Delta = 3000$ cm^{-1}. [18]

Using the theory outlined above, the SOC to only one magnetic sublevel does not enable us to explain the shifts relative to the monomer $\omega_{XY}(+) - \omega_{XY}(\text{monomer}) = -2.9$ MHz and $\omega_{XZ}(+) - \omega_{XZ}(\text{monomer}) = +1.3$ MHz in the ODMR spectrum of the AA phenazine (+ component) dimer. This is because we expect the same dispersion in the XY and XZ transitions, as discussed before. The coupling between the S_1 state and the second triplet $T_2(n\Pi^*)$ located 5000 cm^{-1} above T_1 [18] (which can give a singlet character to the σ_z spin sublevel of T_1 [17] through vibronic spin–orbital mixing) can introduce differences in the dispersion of the transitions. However, this effect is small as evident from the populating and depopulating rates of the lowest triplet state. Unlike naphthalene and TCB, the nitrogen hyperfine coupling constants are quite large and modify the ZFS. Recently it was shown [17e] that the out-of-plane hyperfine matrix element A_{zz} is 28.8 MHz. This and the quadrupole couplings lead into several bands in the ODMR spectra similar to the bands shown in Fig. 3 (flanking the main electron spin transition) for the $|D| + |E|$ transition and also to the bands observed by us for the $2|E|$ transition. Thus we must include A_{zz} in our calculation in order to compute the transitions dispersion.

By symmetry A_{zz} mixes σ_x and σ_y. We shall make the following approximations: (a) all other elements will not be included because they are on the order of few MHz; (b) the hyperfine shift (~4 MHz) of the monomer transition in n-heptane d_{16} [17e] is of the same order of magnitude as that in the perdeutero host. This seems to be a good approximation since nitrogen hyperfine effects are local on the molecule; (c) as in the case of 1, 4-dibromomonaphthalene [20] and naphthalene [8] dimers the hyperfine element is one-half the monomer value. With these approximations we now calculate the energies of the monomer and the dimer. The observed -2.9 and $+1.3$ MHz therefore give the following consistent SOC shift:

$$(J'_S - J'_T)|\tau|^2/\Delta'^2 = +5.5 \text{ MHz}. \tag{3.3}$$

This leads, with $\Delta' = 3000$ cm^{-1} and taking $J'_T = -6$ cm^{-1} (see Appendix B), to the values of τ^x shown in Table IV. Two conclusions can be drawn. First, according to this mechanism J'_S of the singlet state could be ±. Second, the dispersion of the XZ transition is the same as the XY as expected for one channel SOC. From the results in Table IV, the values of the SOC parameters (τ^x) seem reasonable, since we know that one-center SOC should dominate the coupling in the case of phenazine. (We ignored intermolecular spin–spin and spin–orbit interactions). It is interesting to note that if we use a value of 10 cm^{-1} for the matrix element [17a] of SOC, then $J'_S = 10$ cm^{-1}, which is a reasonable value. The full hyperfine and SOC treatment in the monomer and dimer will be published later. [21] We hope to provide a more accurate treatment of the hyperfine by using computer diagonalization of the full matrix.

TABLE IV. Calculation of τ^x and τ^x/Δ' as a function of J'_S for isotopically mixed phenazine crystals.

J'_S (cm^{-1})	+10	+20	+30	+50	+100
τ^x/Δ'	3.4×10^{-3}	2.6×10^{-3}	2.2×10^{-3}	1.8×10^{-3}	1.3×10^{-3}
τ^x (cm^{-1})	10.1	7.9	6.7	5.4	3.9

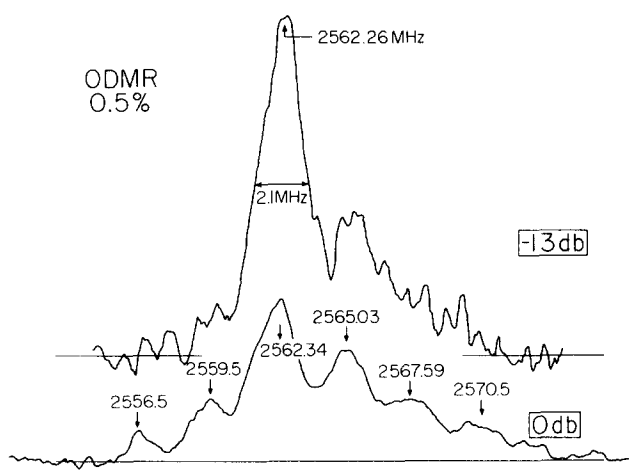

FIG. 3. The ODMR of phenazine-h_8 at two different microwave power levels.

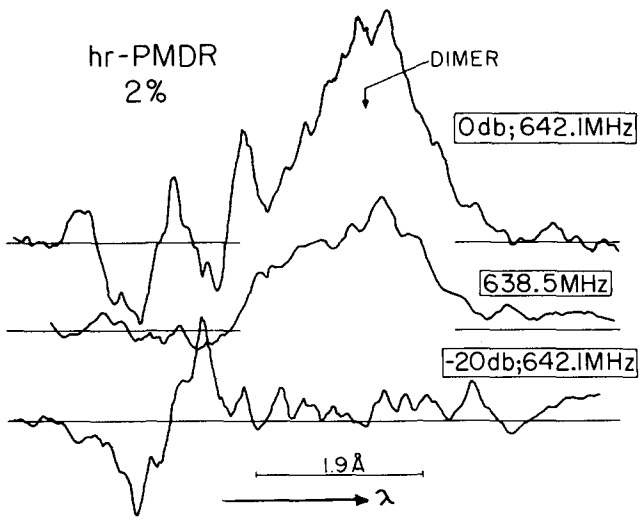

FIG. 4. The high resolution–PMDR spectra of isotopically mixed phenazine crystals at different pump frequencies and powers.

3. PMDR of monomers and dimers: The spin–spin and spin–orbital coupling in the AB small exciton

At 1.5 K, using the 2% crystal, we observed the PMDR transitions by fixing the microwave frequency at the monomer value $\omega(M)$ or at the dimer value $\omega(D)$. The PMDR signals were detected using a lock-in amplifier and a signal averager. Accumulation of traces was essential in some experiments because of the poor signal to noise. Typically, an 80 μ slit (dispersion <5 Å/mm) was used and the microwave power was boosted by a TWT and isolated by at least two isolators in the line. During the spectrometer scan, the microwave frequency was continuously displayed on a digital counter to make sure that the source frequency was stable.

With the microwave frequency at 638.5 MHz, one broad phosphorescence band characteristic of the dimer AA emission was seen at a relatively high microwave power (0 dB). This band can be superimposed on the phosphorescence spectra of the dimer obtained without the microwave source being on. Shifting the microwave frequency to 642.1 MHz (at -20 dB), we observed two peaks opposite in phase to each other (see Fig. 4). At higher power (0 dB), we see these out-of-phase signals and the dimer emission was also seen because of the overlap of the monomer–dimer ODMR resonances at high power broadenings.[22] In our early note,[23] we conjectured on the out-of-phase signal as being due to one of the AB states. We shall quantify this statement more by (i) accurately calculating the ODMR line shape peak positions in the AB dimer states, and (ii) by estimating the relative population in the AA and AB dimers, in order to account for the out-of-phase nature of the signal.

TABLE V. Direction cosines for phenazine crystals.[a]

	X	Y	Z
a'	+0.577	+0.415	−0.704
b	+0.693	+0.202	+0.692
c	+0.432	−0.887	−0.161
X^*	+0.607	+0.349	−0.714
Y^*	+0.388	−0.915	−0.109
$Z^* \equiv b$	+0.693	+0.202	+0.692

[a]The XYZ axis of a molecule in the $a'bc$ crystal frame [Ref. 16(b)] and calculated in the AB dimer frame (this work).

TABLE VI. The AB dimer ODMR transition frequencies of phenazine isotopically mixed crystals.

Transition	Monomer (MHz)[a]	AA dimer (MHz)[a]	Splitting (MHz)
XZ	2562.2	2563.5	+1.3
YZ	1921.3	1925.5	+4.2
XY	640.9	638.0	−2.9
Transition	AB dimer (+ state) (MHz)[b]	AB dimer (− state) (MHz)[b]	Splitting (MHz)
Y^*X^*	770.9	863.0	−92.1
Y^*Z^*	636.8	735.8	−99.0
Z^*X^*	134.1	127.3	+6.8

[a]Experimental. [b]Calculated (see text).

To calculate the expected PMDR spectra of the AB system, we used the result of Sec. II B to compute X^*, Y^*, Z^*. The interaction $J_T = +0.5$ cm^{-1} between the two molecules of the AB phenazine dimer is large enough, compared to the molecular zero-field splittings, so we may describe the spin properties in the axes system of the AB dimer. Using the direction cosines (Table V) the molecules A and B make with the crystal axes (a', b, c) together with the molecular zero-field splittings, the projected dimer spin Hamiltonian onto this system gives in MHz the following zero-field parameters[24]:

$$A' = -311.7\,, \quad B = -185.5\,, \quad C = 496.3\,,$$
$$\alpha_{a'b} = 1190.8\,, \quad \alpha_{bc} = 409.7\,, \quad \alpha_{a'c} = -60.4\,. \tag{3.4}$$

A rotation of $\theta = (\hat{X}^*, \hat{a}') = 4°25$ defines the quantization axes for the dimer $\hat{X}^*$, $\hat{Y}^*$, $\hat{Z}^* \equiv \hat{b}$. The diagonal and symmetric component of the spin Hamiltonian has therefore the following principal values (in MHz)

$$X^* = -316.2\,, \quad Y^* = 500.8\,, \quad Z^* = B\,, \tag{3.5a}$$

and the off-diagonal matrix elements are

$$t_{X^*Z^*} = 1217.9\,, \quad t_{Y^*Z^*} = 320.3\,. \tag{3.5b}$$

Using these values of t and knowing that $J_T = +0.5$ cm^{-1}, we can now calculate the zero-field splittings of the *plus* and *minus* states using perturbation theory [Eqs. (2.11b) and (2.27c) and (2.27d)]. The calculated values are shown in Fig. 5 and Table VI.

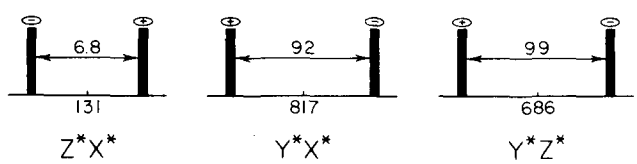

FIG. 5. The three calculated ODMR transitions for the *plus* and *minus* states of the AB dimer of phenazine.

It is clear from these calculations that the *minus* state has a different ODMR frequency ($2|E|$) from the monomer and the AA dimer. However, the *plus* state has one of the transition frequencies very close to the monomer and AA dimer $2|E|$ transitions. So, the observation of the out-of-phase signal at higher energy to the monomer is consistent with our calculation to within 3 MHz. (We cannot evaluate the frequencies of AB any better owing to uncertainties in the direction cosines. These uncertainties influence the center of gravity of the *plus* and *minus* splittings.) Note also that this assignment is in agreement with the ± assignment of factor group states, in Ref. 16, of the pure crystal.

With the procedure outlined in Appendix B we find that the *plus* state stabilization energy in the crystal gives a monomer–dimer splitting of $\sim 0.8\ \mathrm{cm}^{-1}$, indicating that the out-of-phase signal should be located at $+0.8\ \mathrm{cm}^{-1}$ above the monomer. The observed peak splitting is $1-1.5\ \mathrm{cm}^{-1}$, but because there are at least two overlapping (opposite) bands we cannot accurately measure the actual splitting without knowledge of bandwidths and relative intensities. It is interesting to note that, with similar calculation, we expect also the "double monomer"[14] to be at $1.1\ \mathrm{cm}^{-1}$ below the monomer, consistent with a small peak seen in the PMDR spectra. (By double monomer, we mean two guest molecules separated by one host molecule.) Note that the double monomer should have ODMR transitions very close to the A and AA transitions. We do not consider here the PMDR of the *same* aggregates in different environments.

Another way of confirming the assignment of the AB system is to compute the expected emission signal and see if one predicts an opposite trend from that of the AA system. In general, the PMDR signal depends on the population and the radiative rate constant of the two spin levels involved in the transition. We have calculated the transition moment in the AB system using Eq. (2.15) with only the SOC mixing. For example,

$$\mu_{\pm}^{b}\cdot\epsilon=\langle\phi_0\sigma_{s0}|\,\mathbf{M}_A+\mathbf{M}_B\,|{}^3\psi_{\pm}^{b}\rangle\cdot\epsilon$$
$$=-(\lambda^b/\sqrt{2})(\langle\mu_A\rangle\pm\langle\mu_B\rangle)\cdot\epsilon\,. \qquad (3.6)$$

In the case of the AA dimer, the transition moment is simply $\sqrt{2}$ time the molecular one for all the different spin states. For phenazine AB, we find (the radiative decay in the molecule is only through the σ_X state) the following relative radiative rates (square of the transition moments):

$$+\text{ state: } k_{X*}^{r}=0.384\,,\quad k_{Y*}^{r}=0.157\,,\quad k_{Z*}^{r}=0.460\,; \qquad (3.7a)$$

$$-\text{ state: } k_{X*}^{r}=0.353\,,\quad k_{Y*}^{r}=0.144\,,\quad k_{Z*}^{r}=0.500\,. \qquad (3.7b)$$

Now, we note that the transition of the AB dimer at $\approx 1\ \mathrm{cm}^{-1}$ above the monomer (ODMR frequency of 637 MHz) will give an opposite emission signal from the AA and A systems provided that the top level in both cases is more populated. This is because the 637 MHz transition is between σ_{Y^*} and σ_{Z^*} states (from our calculation) and the radiative rate of the σ_{Z^*} which is located at lower energy from σ_{Y^*} is now larger than that of the top level. One can also calculate the population matrix in the AB system using the direction cosines of Table V, but we do not know the extent to which the AB inequivalent interaction influences the population through spin–lattice relaxation as discussed by SOOS.[25] It will be very interesting to study the AB system in phenazine by using EPR methods similar to that of Wolf and his co-workers.[26]

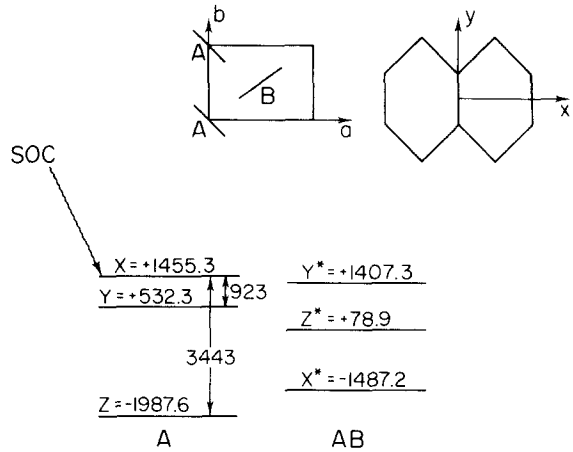

FIG. 6. The ZFS, the coordinate system, and the ordering of the three spin sublevels of naphthalene molecule and of the AB dimer before the perturbation terms were turned on.

It appears therefore that, for the AB phenazine dimer, the most important contribution to the dispersion of the transition frequencies is due to the spin mixing between the *plus* and *minus* states. We can compute the effect of SOC on the dispersion by relating this dispersion of the AB dimer to that of the AA dimer using Eq. (2.35):

$$\omega_{Y*X*}^{+}-\omega_{Y*X*}^{-}=2.4K\,, \qquad (3.8a)$$

$$\omega_{Z*X*}^{+}-\omega_{Z*X*}^{-}=4K+5.3K'\,, \qquad (3.8b)$$

$$\omega_{Y*Z*}^{+}-\omega_{Y*Z*}^{-}=-1.7K-5.3K'\,, \qquad (3.8c)$$

where K and K' are defined in Eq. (2.34).

The value of J_S has been estimated by Hochstrasser[18] to be $<1.25\ \mathrm{cm}^{-1}$. With our estimation for $J_S'=10\ \mathrm{cm}^{-1}$ and $J_T'=-6\ \mathrm{cm}^{-1}$, we compute K and K' [according to Eq. (2.34)], showing that a very small dispersion (≈ 1 MHz) for all the spin transitions in the *plus* and *minus* states is expected.

B. Natpthalene: Spin–spin and spin–orbital dispersions

As for the phenazine crystal, the triplet interactions in naphthalene crystals are two dimensional: $|J_T|=1.2\ \mathrm{cm}^{-1}$[27] for the AB dimer and $|J_T'|=0.5\ \mathrm{cm}^{-1}$[10b] for the AA dimer with the two parallel molecules along the b axis (from calculation) of the crystal. Values of $J_T=-1.2\ \mathrm{cm}^{-1}$ and $J_T'=-0.5\ \mathrm{cm}^{-1}$ were found to reproduce accurately the excitation spectra.[13a,42]

The zero-field transition frequencies of naphthalene molecule isolated in a perdeutero host are[10] (see discussion in Table VIII)

$$\omega_{XZ}=3443\ \mathrm{MHz}\,,\quad \omega_{YZ}=2520\ \mathrm{MHz}\,;\quad \omega_{XY}=923\ \mathrm{MHz}\,. \qquad (3.9)$$

The coordinate system and the ordering of the three spin sublevels are indicated in Fig. 6. These frequen-

cies give the following molecular zero-field splittings (in MHz):

$$X = 1455.3\,, \quad Y = 532.3\,, \quad Z = -1987.6\,. \tag{3.10}$$

Using these zero-field splittings together with the direction cosines of the molecule (Table VII) in the a, b, c' crystal frame, we obtain the following zero-field crystal parameters (in MHz)

$$A = -1068.5\,, \quad B = 78.9\,, \quad C' = 988.6\,,$$
$$\alpha_{ab} = 1022.5\,, \quad \alpha_{bc'} = 181.1\,, \quad \alpha_{ac'} = -1018.1 \tag{3.11}$$

(A, B, and C' do not add exactly to zero because of the insufficient accuracy of the direction cosines). A rotation of $\theta = (X^*, a)$ in the ac' plane defines the zero-order quantization axes of the AB naphthalene which diagonalize H_S^b. With this rotation of $\theta = 22°4$, the principal values of the diagonal symmetric H_S^b spin Hamiltonian become (in MHz)

$$X^* = -1487.2\,, \quad Y^* = 1407.3\,, \quad Z^* \equiv B\,. \tag{3.12}$$

The off-diagonal matrix elements of $H_S^{ac'}$, which couples the triplet spins of the *plus* and *minus* states of the dimer, have the values [using Eq. (2.11b)]

$$t_{X^*b} = 1014.5\,, \quad t_{Y^*b} = -221.4\,. \tag{3.13}$$

Using the value of $J_T = -1.2$ cm^{-1} in Eq. (2.27), the spin–spin perturbation contribution to the zero-field transitions in the *plus* and *minus* states are calculated using the procedure outlined in Sec. II. The results are summarized in Table VIII and Fig. 7. The calculation was done using the direction cosines given in Table VII.

To calculate the effect of SOC, we used the relative radiative rate constants obtained by Sixl and Schwoerer,[28] as we did in phenazine. These relative radiative decay rates from the three magnetic sublevels of isolated naphthalene monomers show that the σ_X component (upper) is predominately active[28] since $k_X^r : k_Y^r = k_Z^r = 1 : (0.1 - 0.2)$.[28b]

TABLE VII. Direction cosines for naphthalene crystals.[a]

	X	Y	Z
a	−0.438	−0.321	+0.840
b	−0.210	−0.872	−0.443
c'	+0.874	−0.370	+0.314
X^*	−0.072 (−0.05998)	−0.438 (−0.41866)	+0.896 (+0.90616)
Y^*	+0.975 (+0.98111)	−0.220 (−0.19200)	−0.029 (−0.02377)
$Z^* \equiv b$	−0.210 (−0.18393)	−0.872 (−0.88762)	−0.443 (−0.42226)

[a]The XYZ axes of a molecule in the abc' crystal frame [Ref. 16(b)] and in the AB dimer frame (this work). The values in parentheses are from Ref. 8(b). Note that King's axes system is different from ours: interchange X^* and Y^*. Our axes system is the same as that of Ref. 26.

TABLE VIII. The calculated contributions of SOC and spin–spin mixing to the ODMR transition frequencies (MHz) of the AB dimer of naphthalene.[a]

Transition	SOC[b]	Spin–spin	Total	Experimental[c]
Y^*X^*	−9.08 (−9.21)	+27.25 (+25.37)	+18.17 (+16.16)	+22.8 ± 2.0
Z^*X^*	+5.27 (+5.16)	−1.36 (−1.02)	+3.91 (+4.14)	+4.1 ± 1.0
Y^*Z^*	−14.35 (−14.36)	+28.61 (+26.39)	+14.26 (+12.03)	+14.5 ± 0.7

[a]We used $J_T = -1.2$ cm^{-1} and the direction cosines given in Table VII (Clarke's values). In parentheses are the calculated values using the direction cosines of King [8(b)].

[b]When k_Z^r/k_X^r or $k_Y^r/k_X^r \to 0$, the Y^*X^* and Y^*Z^* dispersions are similar to the ones given in the table, but Z^*X^* dispersion changes to a relatively small value.

[c]From Ref. 10(b). Note that the sign in the experimental column also depends on the choice for the sign of J'. Our J is negative [taken from Ref. 13(a)], while the sign of J used by Schmidt *et al.* is positive. If we choose J_T to be positive, the signs for the spin–spin dispersions will change uniformly while those for the SOC contribution will still depend on the sign of J_S'. (Also note that using spin–spin coupling alone [see Eq. (2.19), with $|t_{x^*g^*}| \gg |t_{y^*g^*}|$] will not predict the experimental signs for *all* transitions.) The sign of *both* J_T and J_T' should be negative (Ref. 42).

In the first singlet state, the interaction between the two translationally inequivalent molecules of the AB dimers and between the two translationally equivalent molecules (along the b axis) of the AA dimers are $J_S = 15.1$ cm^{-1} and $J_S' = -7.8$ cm^{-1}, respectively.[29] Thus, using Eq. (2.26), we have $K \simeq K' \simeq -2$, assuming that the higher singlet states have similar values of dimer splittings to the lowest one.

The ODMR frequency of the XZ transition in the plus state of the AA dimer is shifted relative to the monomer by 3 MHz.[10b] Assuming that the two ODMR frequencies in the *plus* and *minus* states are shifted symmetrically (from the monomer), we get

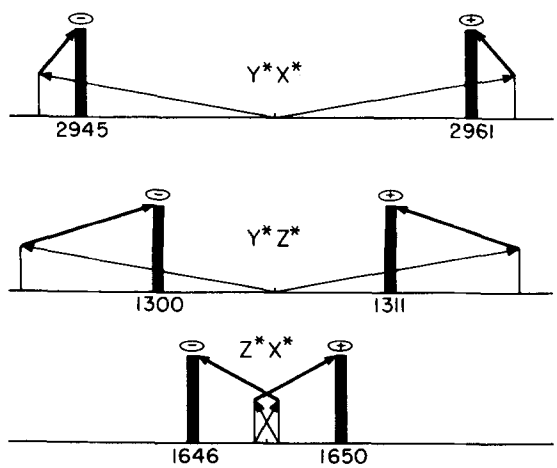

FIG. 7. The effects of spin–spin mixing (—) and SOC (—) on the zero-field transition frequencies in the *plus* (+) and *minus* (−) states of the AB dimer of naphthalene.

TABLE IX. The calculated ODMR transition frequencies (MHz) of the AB dimer of naphthalene.[a]

Transition	+ State (MHz)		− State (MHz)	
Y^*X^*	2961	(2974)	2945	(2951)
Z^*X^*	1650	(1656)	1646	(1652)
Y^*Z^*	1311	(1317.2)	1300	(1303)

[a]The values in parentheses are the experimental numbers. Note that the calculated values given here are obtained after the diagonalization that includes ± interaction matrix elements, $t_{MM'}$.

$$\omega_{XZ}(+) - \omega_{XZ}(-) = (\Delta_X)_{SOC} = -6 \text{ MHz} . \quad (3.14)$$

The dispersion of −6 MHz when used in Eq. (2.35) with $K = K' = -2$, and $k_Z^T/k_X^T = 0.2$, gives for the dispersion of the ODMR transition frequencies of the AB dimer due to the SOC. The values are given in Table VIII.[30]

This simple calculation shows that the contribution of SOC to the dispersion of ODMR frequencies between the *plus and minus* states of the AB dimer could be large! The SOC contribution to the dispersion is different from the contributions due to the off-diagonal matrix elements of the dimer spin Hamiltonian—the latter effect essentially depends on J_T while the spin-orbit contributions (including also the guest-host shift) depend on the relative values of J in the singlet and triplet states.

Finally, using the direction cosines of the molecular axes in the dimer frame as given by King,[8b] we have performed the same calculation (Table IX) to check the effect of direction cosines values on the location of the center of gravity between the *plus* and *minus* states. In both calculations, we can see that the two contributions (SOC and spin-spin) have opposite signs (see Fig. 7). Furthermore, our calculation agrees reasonably well with the experimental values (see Table VIII). Again, the effect of intermolecular spin-spin interaction may even improve the agreement to within 1 MHz, but we feel that this effect is relatively small due to the small value of J. We now conclude this section by mentioning a few words about the molecular SOC. Equation (3.14) assumes that the 6 MHz dispersion in the AA dimer is due to SOC as in TCB (the only mechanism for dispersion in the AA system that we are considering here). Using the values of J_S' and J_T' we obtain $|\tau^x/\Delta|$ of 5.2×10^{-3}. Since the lifetime of naphthalene is longer than TCB (see next section), we expect τ^x of naphthalene to be $\lesssim 10^{-1}$ that of TCB (~ 63 cm^{-1}). In other words, Δ is on the order of 10^4–10^3 cm^{-1}, depending on the choice of J's. To quantify these numbers more we need more facts about the $\sigma\Pi^*$ states of naphthalene. Note that if J_S' and J_T' of these states are known more accurately, the theory presented here should predict the exact SOC parameters and the absolute values of dispersions due to SOC.

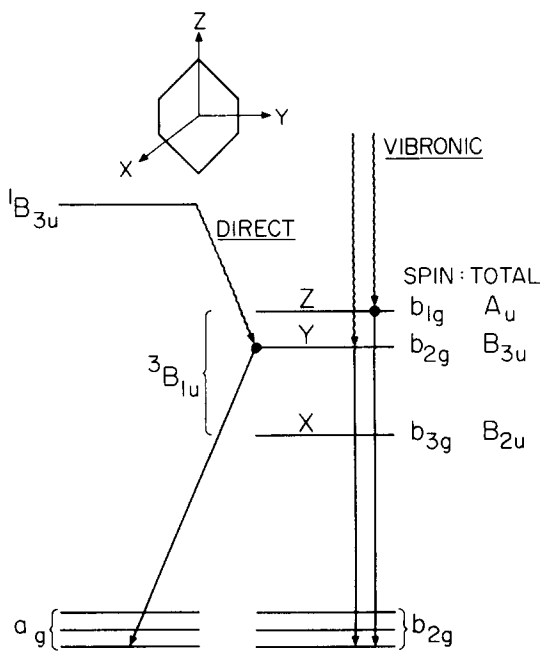

FIG. 8. The coordinate system and the ordering of the three spin sublevels of the lowest triplet state of TCB molecule. This scheme shows the SOC mechanisms (direct and vibronic).

C. Symmetric tetrachlorobenzene

The ordering of the three spin sublevels of the lowest $(\Pi\Pi^*)$[31–36] triplet state of TCB in durene has been established.[31–33] The ordering together with the coordinate system adopted here and the spin-orbit symmetries are summarized in Fig. 8. The analysis of the SOC mechanism in TCB shows (see Fig. 8) that (i) the σ_Y spin sublevel (B_{3u}) *directly* couples by SOC to a singlet state having the B_{3u} symmetry; (ii) the σ_Z and σ_Y spin sublevels (A_u and B_{3u} symmetry, respectively) *indirectly* couple to a B_{2u} singlet state by vibronic-spin-orbit interaction involving the b_{1g} and b_{2g} nontotally symmetric vibration modes; (iii) the effect of SOC on the σ_X (B_{2u} symmetry) spin sublevel is negligible.

The dispersion in the zero-field transition frequencies observed in TCB neat crystals[32b] have been interpreted[32a] by invoking the anisotropy of the SOC into the magnetic sublevels. The ODMR experiments on TCB isotopic mixed crystals[7b] have shown a dispersion for the zero-field transition frequencies in the *plus* and *minus* states of the AA dimers of 7.6 MHz (ZX) and of 5.7 MHz (YX); see Fig. 9. Assuming that only *one* magnetic sublevel in the triplet state is spin-orbitally active does not enable us to reproduce such dispersions. Next, we consider, separately, the contributions to the dispersion of the *direct* spin-orbit coupling and the *vibronic-spin-orbit* interaction.

The populating rates by intersystem crossing (ISC) in

TABLE X. SOC mixing coefficient as a function of J_s' for TCB.

J_s' (cm^{-1})	−1	−5	−10	−15	−20
τ^y/Δ'	7.9×10^{-3}	3.9×10^{-3}	2.8×10^{-3}	2.3×10^{-3}	2.0×10^{-3}

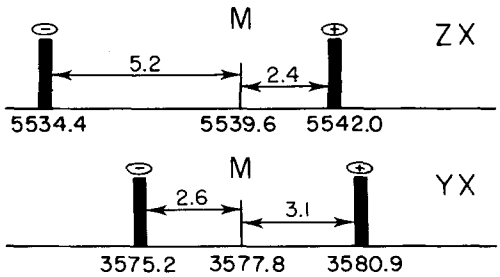

FIG. 9. The experimental dispersion of the ODMR transitions (ZX and YX) for the AA TCB dimer.[7] The ± assignment is *not* unequivocal.

TCB are[31] $P_X : P_Y : P_Z = 1 : 10 : 20$. The relative radiative decay constants for the phosphorescence of isolated TCB in durene are[33] $k_Z^r : k_Y^r : k_X^r = 0 : 19 : < 0.2$ to the totally symsymmetric vibration and $k_Z^r : k_Y^r : k_X^r = 17 : 3.7 : < 0.1$ to the b_{2g} vibrations. Since σ_X does not spin–orbitally couple, we can now conclude that the dispersion in the ZX transition is primarily due to the vibronic–spin–orbital interaction. As we did before, we may use these results [the clear dominance of σ_Y coupling to a_g modes and (0, 0), σ_Z coupling to b_{2g} modes and the ISC to only σ_Y and σ_Z] to calculate the dispersion in the YX manifold. The slight vibronic activity of Y into b_{2g} modes accounts for at most 1.65 MHz (obtained by using the scaling factor 3.7/17).[37] The dispersion in the YX transition due to direct SOC is therefore ~5 MHz. The important point here is that the dispersion for both transitions is caused by different mechanisms. The 7.6 MHz dispersion contains both the vibronic and SOC matrix elements. Hence, using Eq. (2.32), we may write

$$2(J'_S - J'_T)\left|\tau^Y\right|^2/\Delta'^2 = \pm 5 \text{ MHz} , \tag{3.15}$$

where τ^Y is now the matrix element for direct SOC between σ_Y and the singlet manifold (e.g., $\sigma\Pi^*$). It is clear from the above equation that $(J'_S - J'_T)$ must be a negative quantity ($J'_T = +0.34$ cm^{-1}),[32,34] if we take the dispersion in (3.15) to be negative as suggested by the ODMR experiments.[32,7] Using the matrix element for SOC in benzene calculated by Albrecht[38] to be $\simeq 2$ cm^{-1} and knowing that the ratio of benzene-to-TCB lifetimes is ~10^3, we calculate $\tau_{TCB} \simeq 63$ cm^{-1}. This gives $J'_S = -10$ cm^{-1} for $\Delta' = 20\,000$ cm^{-1}, in agreement with the recent location of $^1\sigma\Pi^*$ in benzenes[39] ($S_0 \rightarrow {}^1\sigma\Pi^*$ at 46 000 cm^{-1}). Finally, we have not considered here the AB spin–spin and SOC interactions that we dealt with in phenazine and napthalene AB systems since the Davydov splitting in TCB appears to be very small.[7b,40,41]

IV. CONCLUSION

The ODMR and PMDR studies discussed here for phenazine, naphthalene, and TCB show that several effects are involved in determining the line shape (position) of the ± states of AA and AB small excitons or dimers. These effects include spin–orbital coupling, spin–spin interactions, guest–host energy shifts, and vibronic coupling. We provided expressions for calculating the ODMR frequency dispersions between the ± states when these couplings are operative. The studies show that in contrast with the simple AA dimer case the AB spin–orbital couplings are *multichannel* even though there is only one channel for coupling in the isolated molecule. Expressions relating the AA and AB dispersions are given. Finally, we have applied these theoretical findings to recent experiments and estimated several parameters of interest.

Note added in proof: Very recently, the high (magnetic) field EPR spectra of the AB phenazine dimer has been observed in Professor H. C. Wolf's laboratory in Germany. The preliminary experiments, done on 2% isotopically-mixed crystals, reveal that (a) the average spin Hamiltonian of the AB dimer (Sec. IIB results) is adequate for describing the EPR spectra, and (b) the principal magnetic axes of the AB system are very close to the crystal axes, in agreement with the results of this paper. Also, in the same laboratory, U. Doberer and H. Port have obtained the *excitation* spectra of isotopically-mixed crystals and found that the monomer–dimer splitting is ~4 cm^{-1}, consistent with our earlier emission work.

APPENDIX A: SPIN–ORBITAL COUPLING IN DIFFERENT BASIS SETS

By comparing the electronic resonance matrix elements for the singlet and triplet (J_S and J_T) states to the SOC matrix elements, we had chosen to diagonalize first the dimer electronic Hamiltonian. This diagonalization defines a basis set in which the SOC perturbation is calculated. Instead, we can also use the spin–orbitally perturbed one-site functions as a zero-order basis set and diagonalize the total dimer Hamiltonian. In this Appendix we make connection between the two cases. We consider for the sake of simplicity the AA dimer case with two parallel molecules in which only one triplet spin sublevel is active.

The perturbed one-site function is

$$\left|{}^1\psi^i\right\rangle = (1 - |\lambda|^2)^{1/2}\left|{}^1\phi^i\sigma_s^i\right\rangle + \lambda\left|{}^3\phi^i\sigma_m^i\right\rangle , \tag{A1a}$$

$$\left|{}^3\psi_m^i\right\rangle = (1 - |\lambda|^2)^{1/2}\left|{}^3\phi^i\sigma_m^i\right\rangle - \lambda\left|{}^1\phi^i\sigma_s^i\right\rangle , \tag{A1b}$$

where $\lambda = \tau^m/\Delta$ is the SOC mixing coefficient with τ^m as the matrix element between the singlet and the triplet state, separated in energy by $\Delta = E_0^S - (E_0^T + m)$.

Similarly, the perturbed energies (identical for both molecules) are

$$E_m^T = E_0^T + m - \lambda^2\Delta , \tag{A2a}$$

$$E^S = E_0^S + \lambda^2\Delta . \tag{A2b}$$

Let us define the zero-order functions of the two degenerate states with the excitation localized either on A or B for the singlet state by

$$\left|{}^1\psi^A\phi_0^B\sigma_{s_0}^B\right\rangle \quad \text{and} \quad \left|\phi_0^A\sigma_{s_0}^A\,{}^1\psi^B\right\rangle \tag{A3a}$$

and for the triplet state by

$$\left|{}^3\psi_m^A\phi_0^B\sigma_{s_0}^B\right\rangle \quad \text{and} \quad \left|\phi_0^A\sigma_{s_0}^A\,{}^3\psi_m^B\right\rangle . \tag{A3b}$$

The electronic resonance interaction removes the degeneracy and the matrix element of H_{el}^{AB} between the functions [Eq. (A3b)] becomes

$$V_{AB} = \langle {}^3\psi_m^A \phi_0^B \sigma_{s_0}^B | H_{el}^{AB} | \phi_0^A \sigma_{s_0}^A {}^3\psi_m^B \rangle$$

$$= \langle (1 - |\lambda|^2)^{1/2} {}^3\phi^A \sigma_m^A - \lambda^1 \phi^A \sigma_s^A) \phi_0^B \sigma_{s_0}^B | H_{el}^{AB} |$$

$$\times \phi_A^0 \sigma_{s_0}^A ((1 - |\lambda|^2)^{1/2} {}^3\phi^B \sigma_m^B - \lambda^1 \phi^B \sigma_s^B) \rangle \ , \qquad \text{(A4a)}$$

$$V_{AB} = (1 - |\lambda|^2) J_T' + |\lambda|^2 J_S' \ . \qquad \text{(A4b)}$$

The energy difference of the triplet spin sublevel (say m) between the *plus* and *minus* states of the AA dimer is therefore given by

$$2V_{AB} = 2J_T' + 2|\lambda|^2 (J_S' - J_T') \ . \qquad \text{(A5)}$$

Equation (A5) indicates that the difference in energy between the *plus* and *minus* states of the dimer introduced by the SOC is identical to those derived in Eq. (2.32), to second order:

$$(\Delta_m)_{SOC} = 2|\tau^m|^2 (J_S' - J_T')/\Delta'^2 \ . \qquad \text{(A6)}$$

This connection makes the approach of this work and that of Ref. 7 yield the same results for the AA dimer.

APPENDIX B: EXPRESSIONS FOR THE EFFECT OF GUEST–HOST MIXING ON THE STABILIZATION ENERGIES OF MONOMERS AND DIMERS IN PHENAZINE ISOTOPICALLY MIXED CRYSTALS

In order to show the effect of the guest–host mixing on the monomer energy, we consider the different contributions originating from the nearest neighbors and the next-nearest neighbors (see Fig. 10). Owing to the fact that the most important interaction is between parallel molecules along the b axis, we shall consider first the stabilization energy (X_0) of the monomer by the two nearest neighbors along the b axis. Diagonalization of the energy matrix (3×3) gives

$$X_0 = -2J_T'^2/(\Delta_0 - X_0) \ , \qquad \text{(B1)}$$

where Δ_0 is the zero-order trap depth. Using for phenazine $\Delta_0 = 23$ cm^{-1} and $J_T' = -6$ cm^{-1} gives $X_0 = -2.792$ cm^{-1}. This leads to a trap depth $\Delta = 25.8$ cm^{-1}. Introducing the next-nearest neighbors along the b axis gives, after diagonalization of the energy matrix (5×5),

$$X_0 = -\frac{2J_T'^2}{\Delta_0 - X_0} \frac{1}{1 - J_T'^2/(\Delta_0 - X_0)^2} \ , \qquad \text{(B2)}$$

leading to $X_0 = -2.973$, an extra contribution of 5% to the value of nearest neighbors interactions. This contribution (0.141 cm^{-1}) is large enough to consider the next-next-nearest neighbors (Fig. 10). After diagonalization of the 7×7 matrix, we get the expression

$$X_0 = \frac{-2J_T'^2}{(\Delta_0 - X_0)} \frac{1 - J_T'^2/(\Delta_0 - X_0)^2}{1 - 2J_T'^2/(\Delta_0 - X_0)^2} \ , \qquad \text{(B3)}$$

leading X_0 to a value of -2.941 cm^{-1} (an extra contribution of 0.008 cm^{-1} to the shift). Now, let us consider the contributions due to the four translationally inequivalent host molecules surrounding the monomer (Fig. 10). We get for X_0 the following expressions after diagonalization of the 5×5 matrix:

$$X_0 = \frac{4J_T'^2}{\Delta_0 + J_T' - X_0} \ . \qquad \text{(B4)}$$

With $J_T = +0.5$ cm^{-1} and the above values for Δ_0 and J_T' we get $X_0 = -0.059$ cm^{-1}. It is thus clear that these last contributions to the shift are smaller than the next-nearest neighbors contributions of the parallel molecules but an order of magnitude larger than the next-next-neighbors shifts. Summing on all the different contributions independently (with no cross terms) as indicated in the Fig. 10, we get a total shift of -3 cm^{-1} leading to an expected trap depth of 26 cm^{-1}.

Now, in order to calculate the energy of the lowest symmetric state (optically allowed) of the AA dimer in the mixed crystal, we consider the most efficient coupling of the two molecules with the host. Including the effects of nearest and next-nearest neighbors molecules of the dimer, we get after diagonalization of the 6×6 matrix:

$$X_+ = J_T' - \frac{J_T'^2}{\Delta_0 - X_+} \frac{1}{1 - J_T'^2/(\Delta_0 - X_+)^2} \ . \qquad \text{(B5)}$$

X_+ is the stabilization energy for the lowest symmetric state of the dimer. In Eq. (B5), the first term is the

TABLE XI. Calculation of the guest–host stabilization energy of the monomer (X_0) and the AA dimer (X_+) as a function of Δ_0 (zero-order trap depth) and J'_T.

Δ_0	J_T' [a]	X_0	X_+	Δ Expected
19	−7.30	−4.915	−9.316	23.914
20	−6.92	−4.304	−8.709	24.304
21	−6.62	−3.804	−8.202	24.804
22	−6.40	−3.438	−7.839	25.438
23	−6.21	−3.139	−7.543	26.139
24	−6.06	−2.879	−7.280	26.879
25	−5.93	−2.662	−7.062	27.662

[a] J_T' was calculated (for a given value of Δ_0) to reproduce the observed monomer–dimer splitting of $\delta = 4.4$ cm^{-1}. The last column indicates the expected value for the monomer trap depth in cm^{-1}.

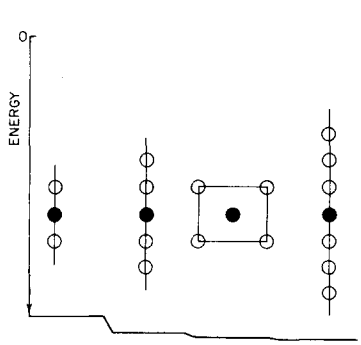

FIG. 10. The stabilization energy of the guest phenazine molecule by the surrounding host molecules. The -2.792 cm^{-1} shift is due to two perdeutero host molecules interacting with a neighboring perproto molecule along the b axis. The -0.141 cm^{-1} shift is due to additional two host molecules along the b axis. Adding two further molecules along the same axis gives only -0.008 cm^{-1} shift. The effect of four (a+b)/2 host molecules is to give a -0.059 cm^{-1} shift. The addition of all these shifts assumes that cross interactions are negligible.

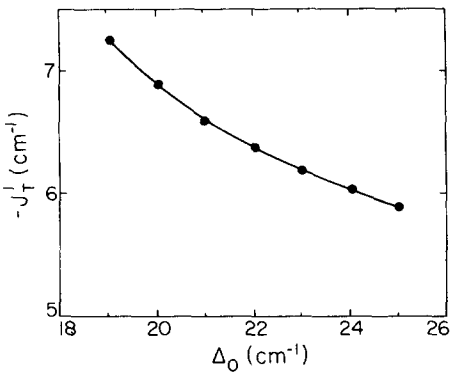

FIG. 11. A plot of the resonance interaction matrix element (J_T') between the two translationally equivalent molecules of the AA phenazine dimer as a function of the zero order trap depth (Δ_0).

interaction between the two molecules of the dimer and the second term contains the stabilization energy due to the nearest neighbors times a correction factor taking into account the next-nearest neighbor molecules.

From the experiment,[14] we know the difference $\delta = X_+ - X_0$ between the energies of the dimer (plus component) and the monomer. Using the expressions of X_+ [Eq. (B5)] and X_0 [Eq. (B3)] calculated above, we obtain the following relationship:

$$\delta = -J_T' - J_T'^2 \alpha/\Delta_0 , \tag{B6a}$$

with

$$\alpha = \Delta_0 \left(\frac{2}{\Delta_0 - X_0} \frac{1}{1 - J_T'^2/(\Delta_0 - X_0)^2} - \frac{1}{\Delta_0 - X_+} \frac{1}{1 - J_T'^2/(\Delta_0 - X_+)^2} \right) . \tag{B6b}$$

The interaction J_T' between the two molecules of the AA dimer is given by the solutions of

$$\alpha J_T'^2 + \Delta_0 J_T' + \delta \Delta_0 = 0 , \tag{B7a}$$

i.e.,

$$J_T' = -(\Delta_0/2\alpha)(1 - (1 - 4\delta\alpha/\Delta_0)^{1/2}) \tag{B7b}$$

δ is known to be equal to 4.4 cm^{-1} for phenazine.[14] For a given zero-order trap depth Δ_0, we start with $J_T' = -6$ cm^{-1} and calculate $\Delta_0 - X_0$, $\Delta_0 - X_+$ leading to α. Then a new value for J_T' can be obtained and so on. The results of these calculations are given in the Table XI for different values of Δ_0 and illustrated in Fig. 11. Larger matrices should be used for more accurate account of the effect of the solid density of states.

[1]A. H. Zewail, J. Chem. Phys. 70, 5759 (1979).
[2]In the systems we are dealing with in this paper (isotopically mixed crystals), the trap depth of the guest is typically 20–200 cm^{-1}. As a result, the guest states are perturbed by the so-called quasiresonance interactions (on the order of J^2/Δ; where Δ is the trap depth and J the coupling matrix element). Hence, when we mention the word dimer, we do not imply a truly isolated pair of molecules since the wave function of the pair is extended on the host. (These quasiresonance interactions are important considerations when treating the line shape functions.) We prefer to call the pair in these cases the small exciton in analogy with the small polaron case. So if we use the word dimers we imply a small exciton.
[3]D. S. McClure, J. Chem. Phys. 20, 682 (1952). See also the paper by W. S. Veeman and J. H. van der Waals, Mol. Phys. 18, 63 (1970).
[4]R. M. Hochstrasser, J. Chem. Phys. 47, 1015 (1967).
[5]H. Sternlicht and H. M. McConnell, J. Chem. Phys. 35, 1793 (1961).
[6](a) R. Silbey, Ann. Rev. Phys. Chem. 27, 203 (1976); (b) D. Burland and A. H. Zewail, Adv. Chem. Phys. 40, 369 (1979).
[7](a) A. H. Zewail and C. B. Harris, Phys. Rev. B 11, 935 (1975); (b) A. H. Zewail and C. B. Harris, Phys. Rev. B 11, 952 (1975).
[8](a) C. A. Hutchison Jr., and J. S. King, Jr., J. Chem. Phys. 58, 392 (1973); (b) J. S. King, Jr., Ph.D. thesis, University of Chicago, Chicago, IL, 1973.
[9]The AA designation should not be confused with dimers made of molecules along the a-crystallographic axis.
[10](a) B. J. Botter, J. Schmidt, and J. H. Van der Waals, Chem. Phys. Lett. 43, 210 (1976); (b) B. J. Botter, A. J. Van Strien, and J. Schmidt, Chem. Phys. Lett. 49, 39 (1977).
[11]J. P. Lemaistre and A. H. Zewail (to be published).
[12]J. P. Lemaistre and Ph. Kottis, J. Chem. Phys. 68, 2730 (1978).
[13](a) J. P. Lemaistre, Ph. Pee, R. Lalanne, F. Dupuy, Ph. Kottis, and H. Port, Chem. Phys. 28, 407 (1978); (b) H. Hong and R. Kopelman, J. Chem. Phys. 55, 724 (1971).
[14]D. D. Smith, D. P. Millar, and A. H. Zewail, J. Chem. Phys. (to be published).
[15]A. H. Zewail, Chem. Phys. Lett. 29, 630 (1974); *ibid.* 33, 46 (1975).
[16](a) R. H. Clarke and R. M. Hochstrasser, J. Chem. Phys. 47, 1915 (1967); (b) R. H. Clarke, Ph.D. thesis, University of Pennsylvania, Philadelphia, PA, 1969.
[17](a) J. Ph. Grivet and J. M. Lhoste, Chem. Phys. Lett. 3, 445 (1969); (b) D. A. Antheunis, J. Schmidt, and J. H. Van der Waals, Chem. Phys. Lett. 6, 255 (1970); (c) D. A. Antheunis, J. Schmidt, and J. H. Van der Waals, Mol. Phys. 27, 1521 (1974); (d) J. Gromer, H. Sixl, and H. C. Wolf, Chem. Phys. Lett. 12, 574 (1972); (e) K. P. Dinse and C. J. Winscom, J. Chem. Phys. 68, 1337 (1978).
[18]R. M. Hochstrasser and C. Marzzacco, J. Chem. Phys. 49, 971 (1968).
[19]U. Eliav and H. Levanon, Chem. Phys. Lett. 36, 377 (1975).
[20]R. M. Hochstrasser and A. H. Zewail, Chem. Phys. 4, 142 (1974).
[21]J. P. Lemaistre and A. H. Zewail (in preparation).
[22]The $|D| + |E|$ transition (XZ) was also studied in a similar manner, but because the difference in the ODMR frequencies between the monomer and the AA dimer (+ component) is smaller than the $2|E|$ (XY), the isolation of the monomer and dimer spectra with the microwave source on was not as complete.
[23]D. D. Smith, R. D. Mead, and A. H. Zewail, Chem. Phys. Lett 50, 358 (1977).
[24]Note the different labelling of axes in naphthalene and phenazine; (ac') vs ($a'c$).
[25]Z. G. Soos, J. Chem. Phys. 51, 2107 (1969).
[26]M. Schwoerer and H. C. Wolf, Mol. Cryst. 3, 177 (1967).
[27](a) D. M. Hanson, J. Chem. Phys. 52, 3409 (1970); (b) C. L. Braun and H. C. Wolf, Chem. Phys. Lett. 9, 260 (1971).
[28](a) H. Sixl and M. Schwoerer, Chem. Phys. Lett. 6, 21 (1970); 2, 14 (1968); (b) one should perhaps use the populating rates as a better indicator of SOC because selection rules for radiative coupling to the ground state may complicate the relationships between the radiative rate constants and SOC. However, the populating rates also suffer from the fact that

the population may visit host or other guest states in its way to the lowest triplet or get scrambled by spin–lattice relaxation.
[29](a) K. E. Mauser, H. Port, and H. C. Wolf, Chem. Phys. 1, 74 (1973); (b) H. Port, D. Vogel, and H. C. Wolf, Chem. Phys. Lett. 34, 23 (1975).
[30]We assume that the different singlet states are essentially at the same energy and have similar J's.
[31]C. R. Chen and M. A. El Sayed, Chem. Phys. Lett. 10, 307 (1971); *ibid.* 10, 313 (1971).
[32](a) A. H. Francis and C. B. Harris, Chem. Phys. Lett. 9, 181 (1971); (b) *ibid.* 9, 188 (1971).
[33]A. H. Francis and C. B. Harris, J. Chem. Phys. 57, 1050 (1972).
[34]D. D. Dlott and M. D. Fayer, Chem. Phys. Lett. 41, 305 (1976).
[35]G. A. George and G. C. Morris, Mol. Cryst. Liquid Cryst. 11, 61 (1970).
[36]M. A. Davidovich, Ph.D. thesis, University of Rochester, Rochester, NY, 1976.
[37]The dispersion and radiative decay rate constants are proportional to $|\tau/\Delta|^2$ provided that we assume that J'_S and J'_T are the same [see Eq. (2.32)] for all channels. Thus, when scaling the dispersion of two transitions according to the relative radiative rates of the spin sublevels involved we must keep in mind the possible difference of J'_S values in the different singlet manifolds.
[38]S. P. McGlynn, T. Azumi, and M. Kinoshita, *The Triplet State* (Prentice-Hall, Englewood Cliffs, NJ, 1969).
[39]M. Ito, H. Abe, and J. Murakami, J. Chem. Phys. 69, 606 (1978), and references therein.
[40]S. Sheng and D. M. Hanson, Chem. Phys. Lett. 33, 451 (1975).
[41]We note that J_T of TCB dimers is small[7] and is closer to ZFS than the naphthalene or phenazine cases. So, some correction to the energies may be obtained if we fully diagonalize the 6×6 energy matrix.
[42]H. Port, private communication.